RESEARCH ARTICLE

EVOLUTIONARY BIOLOGY

Parallel gene expansions drive rapid dietary adaptation in herbivorous woodrats

Dylan M. Klure[1]†, Robert Greenhalgh[1]†, Teri J. Orr[1,2], Michael D. Shapiro[1], M. Denise Dearing[1]*

How mammalian herbivores evolve to feed on chemically defended plants remains poorly understood. In this study, we investigated the adaptation of two species of woodrats (*Neotoma lepida* and *N. bryanti*) to creosote bush (*Larrea tridentata*), a toxic shrub that expanded across the southwestern United States after the Last Glacial Maximum. We found that creosote-adapted woodrats have elevated gene dosage across multiple biotransformation enzyme families. These duplication events occurred independently across species and substantially increase expression of biotransformation genes, especially within the glucuronidation pathway. We propose that increased gene dosage resulting from duplication is an important mechanism by which animals initially adapt to novel environmental pressures.

Herbivores routinely feed on chemically defended plants and thus regularly confront the possibility of being poisoned by their food (*1*). Theory has long predicted that diet selection in herbivores is dictated by hepatic biotransformation ("detoxification") enzymes (*2*). Extensive information about plant-animal interactions exists for arthropods, particularly insects (*3*–*5*). Far less is known about the biotransformation mechanisms used by their mammalian counterparts to metabolize plant compounds, adapt to novel diets, or specialize on toxic plants (*1*, *6*–*10*). Prior research suggests two general mechanisms that enable the metabolism of toxic diets by herbivores: (i) improved catalytic efficiency of biotransformation enzymes through neofunctionalization (*11*) and (ii) higher dosage of biotransformation enzymes through gene duplication (*12*). Since most mammalian species are herbivorous to some extent (*13*), the identification of these mechanisms and their evolution is critical to understanding dietary shifts that enable exploitation of new food resources as well as predicting the response to shifts imposed by changing flora under natural and anthropogenic processes.

We investigated the evolution of dietary adaptation in mammalian herbivores by focusing on woodrat species (*Neotoma* spp.) that experienced a climate-related event with dietary consequences—the extirpation of their primary food resource, juniper (*Juniperus* spp.) and its replacement by creosote bush (*Larrea tridentata*) (Fig. 1A). These floristic changes substantially altered the diet of herbivorous woodrats as recorded in their paleocaches (*14*). Juniper and creosote bush produce disparate plant secondary compounds (terpenes versus phenolics and lignans, respectively) that require different suites of biotransformation enzymes (*1*, *15*, *16*). The dietary shift to creosote occurred independently in two species of woodrats (*Neotoma lepida* and *N. bryanti*) at the end of the Last Glacial Maximum (~19 to 15 thousand years ago), when the American Southwest underwent a natural climate change event (Fig. 1B) (*14*, *17*, *18*). Warming led to the extirpation of juniper, enabling creosote bush, a novel species in the region, to invade (*17*). Currently, *Larrea*

[1]School of Biological Sciences, University of Utah, Salt Lake City, UT, USA. [2]Department of Biology, New Mexico State University, Las Cruces, NM, USA.
*Corresponding author. Email: denise.dearing@utah.edu
†These authors contributed equally to this work.

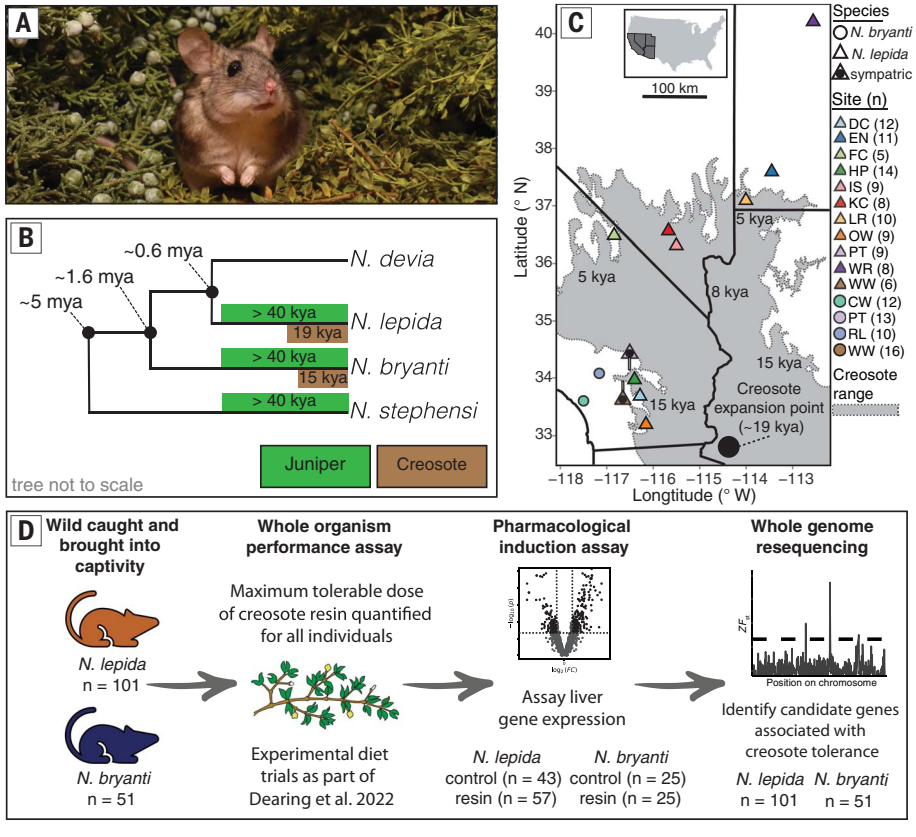

Fig. 1. Woodrat evolutionary history with creosote bush. (**A**) Adult female *N. lepida* between juniper (left; the ancestral diet) and creosote bush (right; the novel diet for this species). [Photo: M. Doolin] (**B**) Phylogenetic relationship of *N. lepida* and *N. bryanti*, and their historical exposure to juniper and creosote bush. Exposure timelines are based on radiocarbon dating of plant material from woodrat paleomiddens (*14*). mya, million years ago; kya, thousand years ago. (**C**) Map of the southwestern United States showing trapping locations of woodrats and the contemporary range of creosote bush (creosote vector provided by the USGS-SVSC-Colorado Plateau Field Station). Creosote expanded across the southwestern United States at the end of the Last Glacial Maximum from a putative refugia near Welton Hills, Arizona (*17*). Approximate dates (kya) are provided on the creosote overlay to demonstrate when creosote arrived at different regions of the Mojave Desert. (**D**) Overview of the experimental approaches used in this study to identify adaptations underlying creosote tolerance in these species. Woodrats were previously phenotyped for creosote tolerance, and the same individuals were used in this study to generate gene expression and whole-genome resequencing datasets.

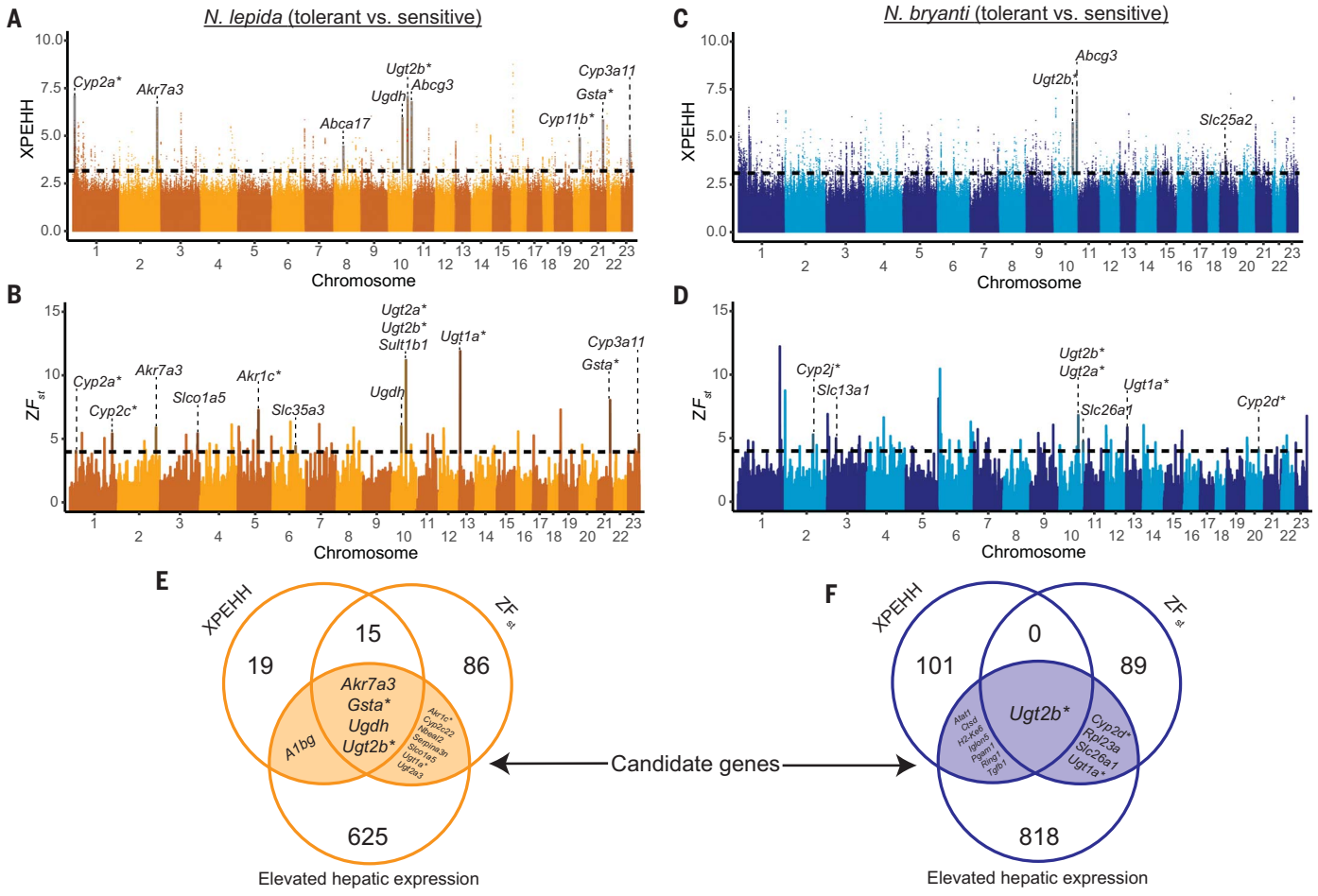

Fig. 2. Genomic regions that contain biotransformation-related genes with signatures of recent positive selection in tolerant individuals. (**A** and **B**) Tolerant *N. lepida* and (**C** and **D**) tolerant *N. bryanti* harbored multiple genomic regions with signatures of recent positive selection, as estimated from cross-population extended haplotype homozygosity (XPEHH) and allele frequency differentiation (ZF_{st}) scans that contain biotransformation genes compared with conspecifics that were sensitive to creosote toxins. Dashed lines indicate the genome-wide significance threshold. Several of the candidate genes under positive selection in (**E**) tolerant *N. lepida* and (**F**) tolerant *N. bryanti*. Asterisks denote instances where candidate genomic regions contained multiple genes belonging to the same subfamily.

species occupy millions of hectares across the Americas (Fig. 1C), and under climate change models, *L. tridentata* is projected to substantially extend its range northward within decades (*19*–*22*). Its leaves are heavily defended by a complex resin of hundreds of chemicals (primarily phenolics and lignans) in substantial quantities making up 10 to 25% of its dry mass (*15*). Few herbivores, including arthropods, have overcome the defenses of this abundant shrub (*15*); however, some *N. lepida* populations ingest large quantities of creosote, particularly during the winter months (*23*, *24*). The recent characterization of the response in one *N. lepida* population capable of ingesting the equivalent of 100% creosote revealed induction of multiple biotransformation genes (*25*). Building on this work, we used a combination of evolutionary, genomic, and experimental approaches to evaluate the two general mechanisms hypothesized to enable toxin metabolism in mammalian herbivores and to identify the portfolio of biotransformation genes under selection in woodrats that feed on creosote (Fig. 1D).

Genes under selection in creosote-tolerant woodrats

Individuals of *N. lepida* and *N. bryanti* exhibit differential tolerance to creosote bush, where those within its range have substantially higher tolerance (*24*). We capitalized on these established phenotypic differences to identify genes under differential selection in woodrats that enable creosote tolerance. Using tissues of animals previously phenotyped for creosote tolerance (*24*), we performed whole-genome resequencing on individuals of *N. lepida* (n = 101) and *N. bryanti* (n = 51) from 13 localities (Fig. 1, C and D, and table S1), achieving 10.9 ± 1.8× (SD) mean genome coverage. Genetic differentiation between localities within each species was consistent with isolation by distance rather than evidence for discrete local populations (fig. S1 and table S2). Estimated genome-wide divergence between species (1.2%) is similar to previous estimates (*26*), with a divergence time of ~1.6 million years ago (*27*) (fig. S1B). These results are consistent with recent expansion events for these species after periods of glaciation (*27*).

Based on previously determined phenotypic tolerance to creosote resin, we categorized individuals as "tolerant" or "sensitive" (*24*) and performed selection scans to identify candidate genomic regions specific to tolerant individuals. We tested for differential genomic signatures of positive selection between creosote-tolerant and creosote-sensitive populations by comparing patterns of extended haplotype homozygosity and allele frequency differentiation (ZF_{st}, where Z is the standard score and F_{st} is the fixation index) using a sliding window approach. We controlled for false-positive differentiation signals using 1000-fold permutation with randomized placement of individuals to the tolerant or sensitive groups (fig. S2). Tolerant *N. lepida*

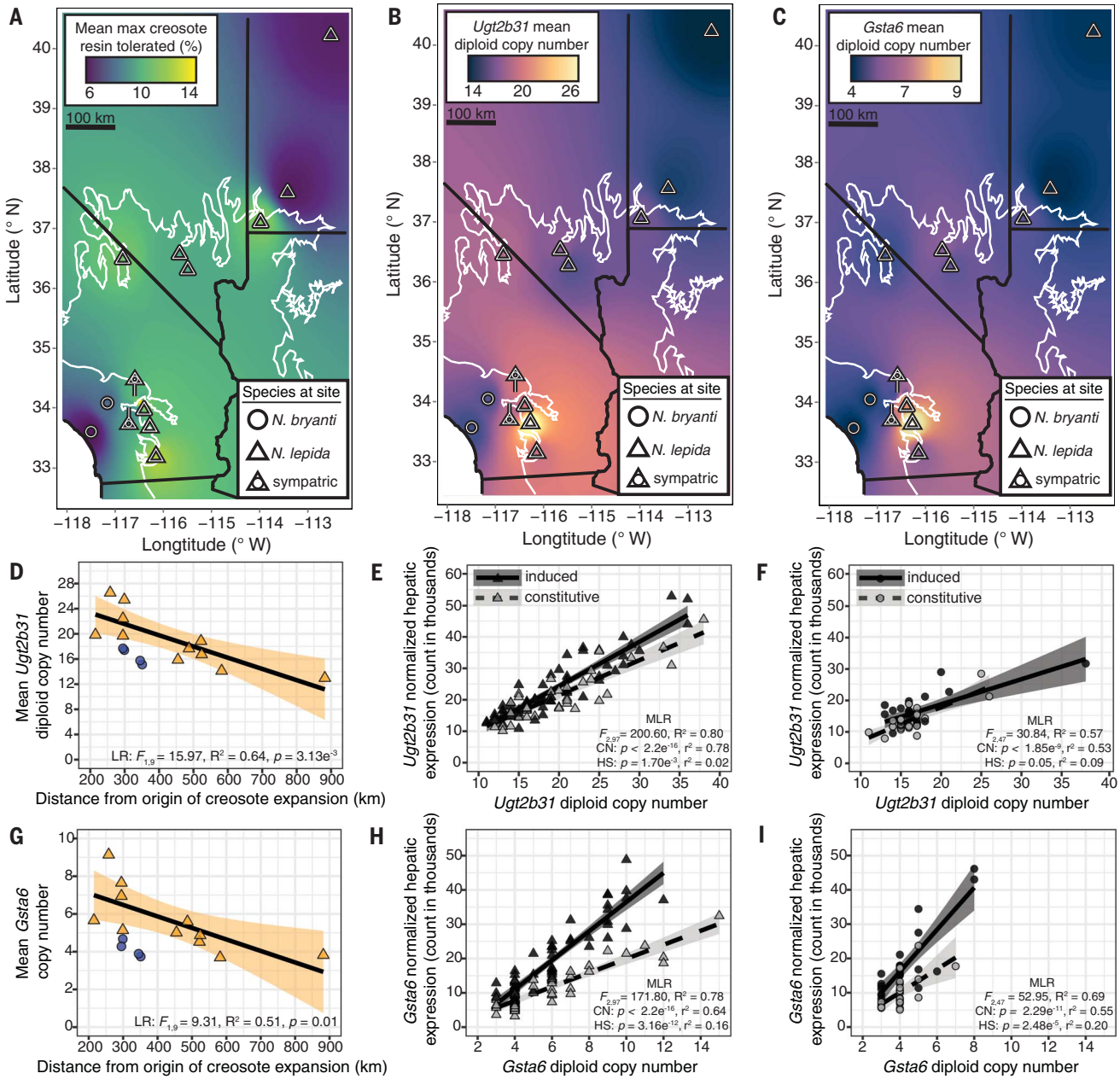

Fig. 3. Tolerance and gene copy number variation are associated with historical exposure to creosote bush. (**A**) Interpolation map of the site-average maximum dose of creosote resin tolerated by captive woodrats. Tolerance was far greater in woodrats sampled from within the distribution of creosote bush (outlined in white). (**B**) *Ugt2b31* and (**C**) *Gsta6* CNV followed a similar pattern to tolerance and was greatest in woodrats sampled from within creosote bush habitat. (**D**) For *N. lepida*, the estimated diploid copy number of *Ugt2b31* was negatively correlated with each sampling site's geographic distance to the putative origin of creosote bush expansion in the United States (Welton Hills, Arizona). Shaded areas represent 95% confidence intervals. *Ugt2b31* individual copy variation was strongly associated with individual hepatic constitutive (control diet) and induced (creosote diet) expression for both (**E**) *N. lepida* and (**F**) *N. bryanti*. *Gsta6* (**G**) CNV and hepatic expression for both (**H**) *N. lepida* and (**I**) *N. bryanti* demonstrated similar patterns to that of *Ugt2b31*. Individual regression coefficients (r^2) for copy number (CN) and hepatic state (HS) shown in (E), (F), (H), and (I) were calculated using a leave-out-one approach.

showed signatures of positive selection in regions containing numerous genes involved in hepatic xenobiotic biotransformation (Fig. 2, A and B). These included multiple aldo-keto reductases (AKRs), monooxygenases (P450s), glutathione *S*-transferases (GSTs), and uridine diphosphate (UDP)–glucuronosyltransferases (UGTs; tables S3 and S4). One candidate region contained UDP-glucose 6-dehydrogenase (*Ugdh*), a gene whose protein product catalyzes the synthesis of the donor substrate used by glucuronosyltransferases (*28*). Similarly, putative selected regions in tolerant *N. bryanti* genomes contained genes encoding biotransformation enzymes in the P450 and UGT families as well as a diverse suite of other functions, including numerous olfactory receptors and several immune genes (Fig. 2, C and D, and tables S5 and S6). While selected regions yielded partially overlapping functional categories of genes related to the processing of toxins, overall, there were a far greater number of putative positive selection events around biotransformation genes among the creosote-tolerant *N. lepida*

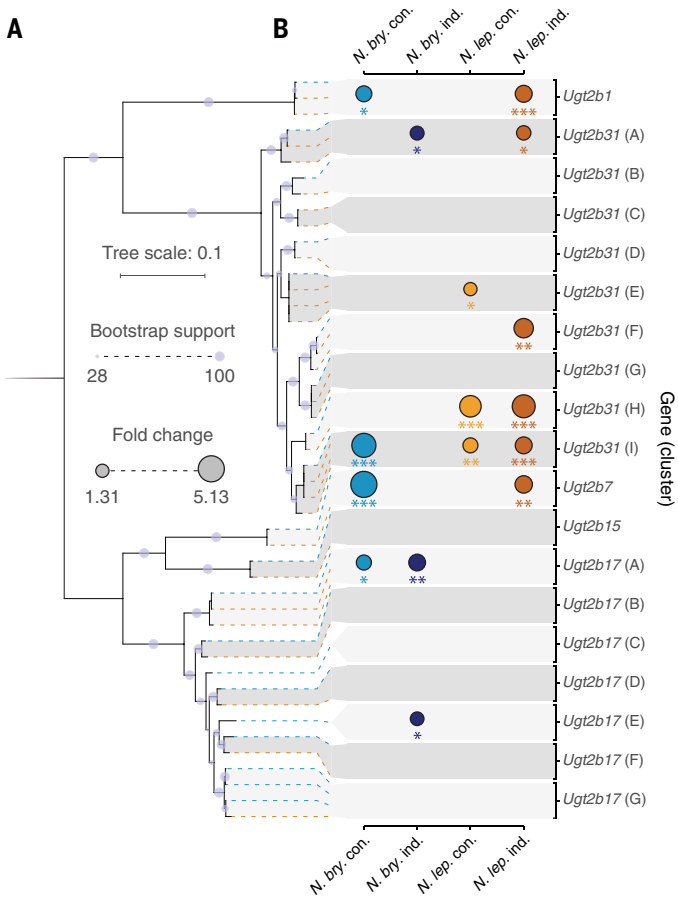

Fig. 4. Phylogeny and expression patterns of genes within the *Ugt2b* array. (**A**) Phylogeny of *Ugt2b* genes reconstructed from coding sequences in the *N. bryanti* and *N. lepida* reference genomes. Alternating light- and dark-gray backgrounds indicate distinct clusters of genes. Dashed lines indicate genes from *N. bryanti* (blue) and *N. lepida* (orange). Circles on branches denote bootstrap support ranging from 28 to 100; terminal branches without circles indicate genes with identical coding sequences. (**B**) Magnitude of expression change for each gene cluster with significant up-regulation between tolerant and sensitive populations. Constitutive changes are those observed when woodrats were fed a control diet, and induced changes are those observed when woodrats consumed a diet enriched in creosote resin con., constitutive; ind., induced. Fold changes are proportional to the size of the circle. Elevated hepatic expression of *Ugt2b1*, *Ugt2b7*, two clusters of *Ugt2b17* genes (A and E), and two clusters of *Ugt2b31* genes (A and I) is associated with creosote tolerance in *N. bryanti*, whereas *Ugt2b1*, *Ugt2b7*, and five clusters of *Ugt2b31* genes (A, E, F, H, and I) are associated with tolerance in *N. lepida* (*$P \leq 0.05$, **$P \leq 0.01$, ***$P \leq 0.001$) as determined by a pairwise test in DESeq2 using Benjamini and Hochberg correction for multiple testing.

compared with *N. bryanti*, which likely contributes to *N. lepida*'s higher tolerance for creosote bush (*24*).

Candidate genes have elevated hepatic expression in tolerant woodrats

Although whole-genome scans revealed multiple candidate genes with signatures of positive selection in tolerant woodrat populations, some of these differentiated regions could be products of selection for traits unrelated to creosote feeding or of neutral processes. Therefore, we conducted feeding trials followed by liver transcriptome analyses to identify genes either constitutively expressed or induced by ingestion of creosote resin (Fig. 1D). Captive woodrats (*N. lepida*, $n = 101$; *N. bryanti*, $n = 51$) were fed either a nontoxic control diet or creosote resin diet, after which we sequenced liver mRNA, achieving 50 million read pairs per transcriptome. Distinct gene expression patterns were evident between the tolerant and sensitive individuals within each species (fig. S3). For *N. lepida*, several genes in the *Akr7a*, *Cyp2c*, *Gsta*, *Ugt1a*, *Ugt2a*, and *Ugt2b* families, as well as *Ugdh*, had significantly higher expression (≥1.25× fold change; $P \leq 0.01$) in the tolerant individuals feeding on creosote resin (Fig. 2E, figs. S4 to S8, and data S1). *N. bryanti* produced similar results: Several genes in the *Cyp2d*, *Ugt1a*, and *Ugt2b* families had higher expression (Fig. 2F, figs. S4 to S8, and data S2). To focus our effort on biotransformation genes related to local adaptation to creosote feeding, we limited subsequent analyses to biotransformation genes with signatures of positive selection and elevated hepatic expression in tolerant individuals.

The overlapping sets of candidate genes from our whole-genome scans and functional transcriptome analyses (Fig. 2, E and F) have well-described functions related to the hepatic metabolism of xenobiotics—many operate in tandem and have been previously implicated in creosote tolerance (*25*, *29*, *30*). P450s increase the hydrophilicity through the addition of polar groups, yielding reactive oxidative metabolites that can be reduced by AKRs. GSTs and UGTs act directly on xenobiotics, such as phenols (*31*), or further modify metabolites of P450s by conjugation with glutathione or glucuronic acid, respectively, reducing hepatotoxicity and facilitating excretion. P450s and UGTs are the most important biotransformation enzymes in mammals, metabolizing 80 and 20% of drugs in humans, respectively (*32*, *33*). Moreover, P450s and UGTs have undergone large expansions in the genomes of *N. lepida* and *N. bryanti*, with smaller expansions evident in the AKR and GST families (*25*, *26*). There were no nonsynonymous mutations within any of these candidate genes found at a frequency ≥50% in tolerant individuals, potentially a consequence of the recent expansion age. Thus, the duplicated genes are not likely to differ in function. Previous studies collectively implicate these gene families (AKR, GST, UGT, P450) in the metabolism of creosote by woodrats using a variety of approaches, including enzyme activity assays and gene expression assays (*25*, *30*). In particular, the results from whole-organism studies report more than twofold greater urinary excretion of glucuronic acid—the product of UGT enzyme activity—in tolerant woodrats (*34*).

Tolerant woodrats have higher copy number of key detoxification genes

Copy number variation (CNV) of these genes was also associated with creosote ingestion. Both species of woodrats demonstrated proximity-based tolerance to creosote, where individuals from within creosote's range had higher tolerance than those sampled outside its range (Fig. 3A). There was evidence for CNV among candidate genes between tolerant and sensitive individuals. For *N. lepida*, tolerant individuals had a greater copy number of *Akr7a3*, *Gsta1*, *Gsta6*, and *Ugt2b31* (fig. S9). Tolerant *N. bryanti* also had a greater copy number of *Ugt2b31*; however, in contrast to *N. lepida*, they did not have an increased copy number for any other candidate genes (fig. S10). These results indicate that expansions of *Akr7a3*, *Gsta1*, and *Gsta6* in tolerant *N. lepida* are likely species-specific adaptations for creosote feeding.

CNV of *Ugt2b31* and *Gsta6* in *N. lepida* was associated with both historical onset and present-day exposure to creosote (Fig. 3, B and C). We modeled CNV within these genes for each individual and their geographic distance from the putative center of creosote bush expansion (Welton Hills, Arizona) (*17*). Diploid copy number of *Ugt2b31* was inversely correlated with each site's distance to the center of creosote expansion (Fig. 3B), where sites with the longest exposure time had the highest gene copy number. Specifically, *N. lepida* sampled closest to the center had approximately nine more *Ugt2b31*

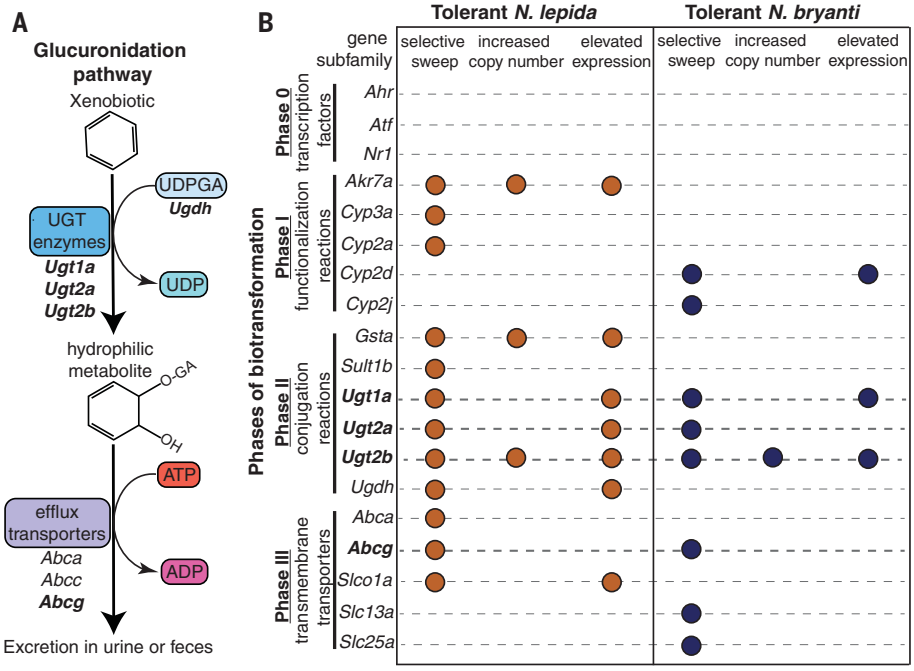

Fig. 5. Overview of candidate hepatic biotransformation genes associated with creosote tolerance. (**A**) The glucuronidation pathway is an important phase II biotransformation process that has undergone considerable and independent evolutionary change in tolerant *N. lepida* and *N. bryanti* (relevant gene subfamilies in bold). Specifically, tolerant individuals of both species exhibited increased gene dosage of *Ugt2b* genes and shared selective sweeps around efflux transporter *Abcg3*. Additionally, tolerant *N. lepida* had signatures of positive selection around single-copy gene *Ugdh* with both elevated constitutive and induced hepatic expression. The protein product of this gene catalyzes the synthesis of uridine 5′-diphosphoglucuronic acid (UDPGA), the donor molecule of glucuronic acid, and is a rate-limiting step of glucuronidation. ATP, adenosine triphosphate; ADP, adenosine diphosphate. (**B**) Gene subfamilies are organized according to the phase of biotransformation (shown on the left). Within creosote-tolerant individuals, circles denote whether a gene subfamily had differential signatures of positive selection, increased copy number, and/or elevated expression (either constitutively, induced, or both) relative to sensitive conspecifics. Gene subfamily names in bold had independent signatures of positive selection across species.

copies than did those furthest away. This model supports a rate of expansion of approximately three additional *Ugt2b31* copies per 5000 years of creosote exposure (Fig. 3D). *N. bryanti* demonstrated a similar pattern, where individuals sampled closest to the geographic origin of creosote had two additional *Ugt2b31* copies (Fig. 3D). Expansions of *Ugt2b31* in tolerant *N. lepida* and *N. bryanti* were associated with greater constitutive and inducible hepatic expression (Fig. 3, E and F). *Gsta6* CNV and expression demonstrated similar patterns (Fig. 3, C and G to I). Thus, for creosote-tolerant woodrats, length of exposure to creosote is associated with large-scale expansions of *Ugt2b31* and, to a lesser extent, *Gsta6*, supporting the hypothesis that these expansions are adaptive for creosote feeding. *N. stephensi*, a close relative and a juniper specialist, has fewer copies of *Ugt2b* and *Gsta* genes compared with creosote-tolerant *N. lepida* and *N. bryanti* individuals (figs. S11 and S12), further indicating that creosote feeding selected for increased copy number of these genes.

Glucuronidation plays a key role in creosote tolerance

The finding that adaptations within the *Ugt2b* family may underlie creosote bush feeding in woodrats is consistent with its critical role in xenobiotic metabolism in mammals (*35*, *36*). Notably, while dietary creosote induced expression of most *Ugt2b* genes, the magnitude of induction for *Ugt2b31* genes was often lower than constitutive differences observed between tolerant and sensitive populations (figs. S6 to S8). This pattern strongly suggests that *Ugt2b31* expression in woodrats is dictated primarily by gene dosage rather than by regulatory elements such as xenobiotic sensing nuclear receptors. Individual CNV of *Ugt2b31* explained 78% of the variation in hepatic expression on creosote resin diets (Fig. 3C). To further examine expression dynamics of copy number–variable UGTs, we performed phylogenetic reconstruction of *Ugt2b* genes in both reference genomes and evaluated transcription at the level of gene clusters to see whether closely related genes shared similar constitutive or induced expression patterns across populations and species (Fig. 4 and figs. S6 to S8). Regardless of species, tolerant populations exhibited elevated expression in *Ugt2b1*, *Ugt2b7*, and the *Ugt2b31* gene clusters A and I. Furthermore, within the *Ugt2b31* clusters, *N. lepida* tolerance was linked to elevated expression in gene clusters E, F, and H, whereas in *N. bryanti*, tolerance was associated with heightened expression of the *Ugt2b17* gene clusters A and E.

The features identified across the *Ugt2b* family are consistent with repeated and independent expansion events in both species in response to the invasion of creosote. Several lines of evidence support the role of parallel evolution in the history of this gene family. First, *Ugt2b* gene expansions are similar in tolerant *N. lepida* and *N. bryanti,* closely mirroring historical estimates of creosote exposure. These expansions have increased overall dosage of *Ugt2b* genes relative to closely related species (fig. S12) (*37*–*40*). Second, both woodrat species exhibit species-specific haplotypes across the *Ugt2b* family (fig. S13), indicating that interspecific introgression is unlikely to have played a role in this gene family's evolution. Finally, within tolerant individuals, there have been additional species-specific expansions of the *Ugt2b* family linked to distinctive expression patterns (Fig. 4). We propose that the recent independent *Ugt2b* expansion events in tolerant populations were prompted by the expansion of creosote driving copy number to exceptionally high levels reaching as many as ~38 putative copies of *Ugt2b31* in some individuals (Fig. 3E) and, consequently, elevated expression of these genes. This notable increase in gene dosage bolsters the liver's capacity for glucuronidation.

Further evidence for the importance of the glucuronidation pathway in mediating creosote tolerance was apparent in *Ugdh* and *Abcc3*. *Ugdh* catalyzes the rate-limiting step of the glucuronidation pathway (Fig. 5A). Although *Ugdh* is a single-copy gene in both species (figs. S9 and S10), tolerant *N. lepida* exhibited a distinctive haplotype (fig. S14) and had elevated expression levels of *Ugdh* regardless of diet (fig. S5). Elevated expression in tolerant individuals represented elevated protein levels (fig. S15). Since no nonsynonymous changes were present in the coding sequence, the tolerant haplotype likely includes a regulatory change responsible for enhanced expression. *Abcc3* encodes the multidrug resistance 3 (MRP3) transporter, one of the major exporters of glucuronidated metabolites from the liver (Fig. 5A) (*41*). *Abcc3* was consistently among the most differentially expressed genes (data S1 and S2), exhibiting a minimum induction of 2.8× on a resin diet regardless of species (fig. S16). As *Abcc3* expression correlates with the rate at which glucuronidated compounds are effluxed from the liver (*42*), up-regulation of this transporter further

reinforces the importance of the glucuronidation pathway in mediating creosote tolerance.

We did not detect expansions of functionalization enzymes (e.g., P450s) in tolerant individuals; however, this result does not imply that these enzymes do not contribute to creosote resin metabolism. *Cyp3a11* and *Ephx1*, for example, are duplicated in both species and highly expressed in the liver on a resin diet regardless of species identity or tolerance (fig. S17) (*25*). Given that these duplications in *Neotoma* are present in all sequenced woodrat species, these functionalization enzymes likely represent ancestral mechanisms for herbivory.

Genomic features associated with creosote tolerance were evident only in individuals sampled from within creosote's distribution, despite evidence for high levels of intraspecific gene flow. Thus, we hypothesize that expansions in the *Ugt2b* family could result in fitness costs at sites where creosote is not regularly encountered. Specifically, the high constitutive expression of *Ugt2b* and *Ugdh* in tolerant individuals may have a fitness cost related to the demands of maintaining high enzyme levels or loss of glucose molecules to the conjugate, uridine 5′-diphosphoglucuronic acid (*28*) (Fig. 5A). Such costs could be maladaptive for woodrats outside creosote's range but could represent an adaptive trade-off when creosote is a major dietary component.

Another major finding of this work is the role of gene duplication in facilitating rapid dietary adaptation. A large body of evidence demonstrates that biotransformation gene expansion enables arthropod herbivores to feed on toxins both natural and anthropogenic (*3*–*5*). In contrast, although expansions of hepatic biotransformation genes have been noted in vertebrates (*12*, *43*), there has been relatively little focus on how these are tied to evolutionary mechanisms associated with herbivory. Here, we find that the independent adaptation of two woodrat species to a novel and toxic diet is associated with expansion of liver biotransformation enzyme families, akin to the mechanisms that underlie dietary adaptation in arthropods. In addition, of the two potential genetic mechanisms thought to enable herbivory in mammals, we only found evidence for one of them. There was no support for selection for neofunctionalization within the expanded biotransformation enzyme families, as the few nonsynonymous mutations we detected across paralogs were rare, potentially a consequence of the recent age of these expansions. Instead, we find that variation in gene dosage enabled by duplication likely plays a critical role in creosote tolerance. The potential immediate benefits of increased gene dosage without neofunctionalization are often overlooked (*44*). This mechanism of local adaptation to environmental toxins by means of quantitative differences in biotransformation gene dosage may be common in other vertebrate herbivores, as indicated by recent genomic surveys (*36*, *45*), and might be a general mechanism by which species with longer generation times rapidly adapt to novel food sources as well as other aspects of environmental change (*46*, *47*).

For more than half a century, biologists have speculated which evolutionary mechanisms enable mammalian herbivores to exploit novel and toxic foods (*2*). Decades of debate have centered on the relative role of protein changes and quantitative differences in the dosage of biotransformation genes as well as the impact of their transcriptional regulators. Here, we identify the portfolio of biotransformation genes and their evolution associated with rapid dietary adaptation in mammalian herbivores. The ability of woodrats to feed on creosote bush is one of a growing number of examples of rapid local adaptation in vertebrates (*48*–*50*).

REFERENCES AND NOTES

1. M. D. Dearing, W. J. Foley, S. McLean, *Annu. Rev. Ecol. Evol. Syst.* **36**, 169–189 (2005).
2. W. J. Freeland, D. H. Janzen, *Am. Nat.* **108**, 269–289 (1974).
3. J.-C. Simon *et al*., *Brief. Funct. Genomics* **14**, 413–423 (2015).
4. N. J. Hawkins, C. Bass, A. Dixon, P. Neve, *Biol. Rev. Camb. Philos. Soc.* **94**, 135–155 (2019).
5. H. M. Heidel-Fischer, H. Vogel, *Curr. Opin. Insect Sci.* **8**, 8–14 (2015).
6. W. J. Foley, G. R. Iason, C. McArthur, in *Nutritional Ecology of Herbivores: Proceedings of the Vth International Symposium on the Nutrition of Herbivores*, H.-J. G. Jung, G. C. Fahey Jr., Eds. (American Society of Animal Science, 1999), pp. 130–209.
7. K. J. Marsh, I. R. Wallis, R. L. Andrew, W. J. Foley, *J. Chem. Ecol.* **32**, 1247–1266 (2006).
8. J. S. Sorensen, M. D. Dearing, *J. Chem. Ecol.* **32**, 1181–1196 (2006).
9. J. S. Sorensen, M. M. Skopec, M. D. Dearing, *J. Chem. Ecol.* **32**, 1229–1246 (2006).
10. B. D. Moore, N. L. Wiggins, K. J. Marsh, M. D. Dearing, W. J. Foley, *Anim. Prod. Sci.* **55**, 272 (2015).
11. Z. Wen, S. Rupasinghe, G. Niu, M. R. Berenbaum, M. A. Schuler, *Mol. Biol. Evol.* **23**, 2434–2443 (2006).
12. M. Ingelman-Sundberg, *Pharmacogenomics J.* **5**, 6–13 (2005).
13. S. A. Price, S. S. B. Hopkins, K. K. Smith, V. L. Roth, *Proc. Natl. Acad. Sci. U.S.A.* **109**, 7008–7012 (2012).
14. J. L. Betancourt, T. R. Van Devender, P. S. Martin, Eds., *Packrat Middens: The Last 40,000 Years of Biotic Change* (Univ. of Arizona Press, 1990).
15. T. J. Mabry, J. H. Hunziker, D. R. Difeo, in *Creosote Bush: Biology and Chemistry of Larrea in New World Deserts*, T. J. Mabry, J. H. Hunziker, D. R. Difeo, Eds. (Academic Press, 1977), pp. 115–134.
16. J. L. Holchek *et al*., *Trop. Grassl.* **24**, 93–98 (1990).
17. K. L. Hunter *et al*., *Glob. Ecol. Biogeogr.* **10**, 521–533 (2001).
18. W. G. Spaulding, in *Packrat Middens: The Last 40,000 Years of Biotic Change*, J. L. Betancourt, T. R. Van Devender, P. S. Martin, Eds. (Univ. of Arizona Press, 1990), pp. 166–199.
19. M. M. Friggens, M. V. Warwell, J. C. Chambers, S. G. Kitchen, in *Climate Change in Grasslands, Shrublands, and Deserts of the Interior American West: A Review and Needs Assessment*, D. M. Finch, Ed., Gen. Tech. Rep. RMRS-GTR-285 (US Department of Agriculture, Forest Service, Rocky Mountain Research Station, 2012), pp. 1–20.
20. S. L. Shafer, P. J. Bartlein, R. S. Thompson, *Ecosystems* **4**, 200–215 (2001).
21. P. V. Wells, J. H. Hunziker, *Ann. Mo. Bot. Gard.* **63**, 843–861 (1976).
22. A. E. Kelly, M. L. Goulden, *Proc. Natl. Acad. Sci. U.S.A.* **105**, 11823–11826 (2008).
23. W. H. Karasov, *Physiol. Zool.* **62**, 1351–1382 (1989).
24. M. D. Dearing *et al*., *Funct. Ecol.* **36**, 2119–2131 (2022).
25. R. Greenhalgh *et al*., *Comp. Biochem. Physiol. C Toxicol. Pharmacol.* **280**, 109870 (2024).
26. R. Greenhalgh *et al*., *Mol. Ecol. Resour.* **22**, 2713–2731 (2022).
27. J. L. Patton, D. G. Huckaby, S. T. Álvarez-Castañeda, *The Evolutionary History and a Systematic Revision of Woodrats of the* Neotoma lepida *Group* (Univ. of California Press, 2007).
28. S. Egger, A. Chaikuad, K. L. Kavanagh, U. Oppermann, B. Nidetzky, *Biochem. Soc. Trans.* **38**, 1378–1385 (2010).
29. C. D. Klaassen, *Casarett & Doull's Toxicology: The Basic Science of Poisons* (McGraw Hill, ed. 9, 2018).
30. E. Magnanou, J. R. Malenke, M. D. Dearing, *Mol. Ecol.* **18**, 2401–2414 (2009).
31. T. R. Tephly, B. Burchell, *Trends Pharmacol. Sci.* **11**, 276–279 (1990).
32. M. Zhao *et al*., *Int. J. Mol. Sci.* **22**, 12808 (2021).
33. R. Fujiwara, E. Yoda, R. H. Tukey, *Drug Metab. Pharmacokinet.* **33**, 9–16 (2018).
34. A. M. Mangione, D. Dearing, W. Karasov, *J. Chem. Ecol.* **27**, 2559–2578 (2001).
35. R. Meech *et al*., *Physiol. Rev.* **99**, 1153–1222 (2019).
36. X. Xing *et al*., *Genomics Proteomics Bioinformatics* **21**, 203–215 (2023).
37. A. D. Long *et al*., *Sci. Adv.* **5**, eaaw6441 (2019).
38. Mouse Genome Sequencing Consortium, *Nature* **420**, 520–562 (2002).
39. Rat Genome Sequencing Project Consortium, *Nature* **428**, 493–521 (2004).
40. N. A. O'Leary *et al*., *Nucleic Acids Res.* **44**, D733–D745 (2016).
41. G. Yang *et al*., *Drug Metab. Rev.* **49**, 105–138 (2017).
42. P. Borst, R. O. Elferink, *Annu. Rev. Biochem.* **71**, 537–592 (2002).
43. E. Lundqvist, I. Johansson, M. Ingelman-Sundberg, *Gene* **226**, 327–338 (1999).
44. F. A. Kondrashov, *Proc. Biol. Sci.* **279**, 5048–5057 (2012).
45. R. N. Johnson *et al*., *Nat. Genet.* **50**, 1102–1111 (2018).
46. J. H. Thomas, *PLOS Genet.* **3**, e67 (2007).
47. K. Guschanski, M. Warnefors, H. Kaessmann, *Genome Res.* **27**, 1461–1474 (2017).
48. R. M. Schweizer *et al*., *PLOS Genet.* **15**, e1008420 (2019).
49. E. M. Oziolor *et al*., *Science* **364**, 455–457 (2019).
50. M. R. Jones *et al*., *Science* **360**, 1355–1358 (2018).

ACKNOWLEDGMENTS

We are grateful to J. Patton, R. Martínez-Mota, L. Mulvey, J. R. Malcolm, M. Skopec, G. Cocke, H. Christensen, W. Kenner, S. R. Stephens, J. Dixon, T. P. Eiting, R. Rusin, E. Rickart, M. Nelson, M. Doolin, S. Weinstein, T. Stapleton, C. Kohlschein, B. Cragun, and N. Armstrong for aid in sample collection, processing, and animal care. We thank E. Symeonidi, T. Karasov, B. Dalley, and the University of Utah High-Throughput Genomics Core for assistance with library preparation and sequencing. We thank the Boyd Deep Canyon Desert Research Center, Orange County Parks, Anza-Borrego Desert Research Center, and the Wildlands Conservancy for assistance with fieldwork. W. Karasov, W. Foley, and A. Hancock provided helpful comments on the initial manuscript and figures. Three anonymous reviewers also contributed suggestions that improved the final manuscript. Animal work was approved under the University of Utah's Institutional Animal Care and Use Committee (protocols 16-02011 and 21-12007) and by California Department of Fish and Wildlife Scientific Collection permits (SC-2105, SC-8123, and S-190880007-20171-001), a Nevada Department of Wildlife scientific collection permit (LN-333663), and Utah Division of Wildlife Resources Collect/Possess/Release permits (5194-1 and 5194-03). The support and resources provided by the Center for High Performance Computing at the University of Utah are gratefully acknowledged. **Funding:** National Science Foundation Integrative Organismal Systems award 1656497 to M.D.D. and M.D.S.; National Science Foundation Independent Research/Development Program (M.D.D.); National Institutes of Health Institutional Training Grant T32GM141848 to D.M.K.; University of Utah Global Change and Sustainability Center Research Award to D.M.K.; University of Utah Graduate School Research Fellowship to D.M.K.; National Institutes of Health Grant RG35M131787 to M.D.S. **Author contributions:** Conceptualization: M.D.S. and M.D.D. Methodology: D.M.K., R.G., T.J.O., M.D.D., and M.D.S. Investigation: D.M.K., R.G., and T.J.O. Visualization: D.M.K. and R.G. Funding acquisition: D.M.K., M.D.S., and M.D.D. Project administration: D.M.K., R.G., T.J.O., and M.D.D. Supervision: M.D.S. and M.D.D. Writing – original draft: D.M.K., R.G., and M.D.D. Writing – review & editing: D.M.K., R.G., T.J.O., M.D.S., and M.D.D. **Competing interests:** The authors declare that they have no competing interests. **Data and materials availability:** Code and supplementary files (including annotations and variant calls) have been deposited with the Open Science Foundation and are available at https://osf.io/4j867/. The *N. stephensi* genome and annotation files have also been deposited with the Open Science Foundation and are available at https://osf.io/zny8f/.

Genome and transcriptome sequencing data have been deposited in the Sequence Read Archive under BioProject PRJNA1101943, and the *N. stephensi* HiFi sequences have been deposited under BioProject PRJNA1148114. The Hoopa transcriptome sequencing data were released as part of a previous study and are available under BioProject PRJNA1002292.

SUPPLEMENTARY MATERIALS

Submitted 11 April 2024; accepted 15 November 2024
10.1126/science.adp7978